THE PERFORMANCE OF HYDROLOGICAL MONTHLY PRODUCTS USING SSM/I – SSMI/S

11B.3   **SENSORS**

Daniel Vila[1,2], Cecilia Hernandez[2], Ralph Ferraro[3], Hilawe Semunegus[4]
[1] Instituto Nacional de Pesquisas Espacias – Centro de Previsão do Tempo e Estudos Climaticos
[2] Cooperative Institute of Climate and Satellites - MD
[3] NOAA/NESDIS
[4] NCDC/NOAA

1. INTRODUCTION

Global monthly rainfall estimates and other hydrological products have been produced from 1987 to present using measurements from the Defense Meteorological Satellite Program (DMSP) series of Special Sensor Microwave Imager (SSM/I). The DMSP F16 satellite was successfully launched on October 18, 2003, carrying onboard the first Special Sensor Microwave Imager/Sounder (SSMI/S) followed by DMSP F17 and F18 launched in 2009 and 2010 respectively. SSMI/S imaging channels maintain similar resolution and spectral frequency to the SSM/I except 91.655 GHz on SSMI/S vs. 85.5 GHz on SSM/I. Additionally, the SSMI/S added a new 150 GHz channel plus three humidity profiling channels, which consists of pairs of narrow passbands on either side of the H_2O absorption line center at 183.3 GHz similar to those on the Advanced Microwave Sounding Unit–B/ Microwave Humidity Sounder (AMSU-B/MHS) instruments. A wider swath, approximately 1700 km for SSMI/S compared with only 1400 km for SSM/I, is also a new characteristic of this instrument.

This research has two objectives: The reprocessing of the existing SSMI database using an improved QC scheme for antenna temperatures (Vila et al., 2010) for the entire SSM/I period (1987-2009) and the continuation in monitoring and retrieving of atmospheric and surface parameters such as precipitation (Ferraro, 1997), sea ice, cloud liquid water (Alihouse et al, 1990) among other products using SSMI/S measurements.

These products, combined with those derived from other passive microwave sensors such as AMSU/MHS onboard NOAA satellites, offer the scientific community an excellent source of global hydrological products. The high temporal frequency of rainfall retrievals and other hydrological products will also help to better understand the diurnal cycle for different climate regimes around the world (Vila et al., 2007).

This paper is organized as follows: in section 2 a brief description of the data used in this research and a brief description of the improved QC scheme for SSMI is presented. The antenna temperature calibration methodology for SSMI/S using a histogram matching technique will be discussed in section 3. Time series analysis and some comparisons between SSM/I F-13 and SSMI/S F-17 products will be presented in section 4.

2. DATA AND ALGORITHMS

2.1. DATA SOURCES

For this particular project, SSM/I and SSMI/S Temperature Data Record (TDR) files from Comprehensive Large Array-data Stewardship System (CLASS) were used. CLASS is a web-based data archive and distribution system for NOAA's environmental data. TDRs contain calibrated and earth-located data prior to irreversible antenna pattern correction. The temperature data represent microwave energy levels measured by the radiometer instrument. The energy levels are expressed as an equivalent blackbody temperature (antenna temperature, AT hereafter). More information about SSM/I and SSMI/S TDR files used in this study can be found in the NOAA National Climatic Data Center web page (http://www.ncdc.noaa.gov/oa/rsad/ssmi/ssmi.html). These files have been mapped to 1/3° lat x 1/3° long linear daily grids for the ascending and descending nodes respectively. This method was established in the early stages of GPCP and must be maintained for continuity of the GPCP V2 global rainfall products, however, it is recognized that a superior product could be developed using the highest resolution data. For this study, we have used all available data from F-08, F-11 and F-13 satellites. In case of F-17, only seven channels were remapped to daily grids to match with the correspondent channels of SSM/I sensor. SSMI/S imaging channels maintain similar

resolution and spectral frequency to the SSM/I except 91.655 GHz on SSMI/S vs. 85.5 GHz on SSM/I as it was mentioned in the introduction

2.2. IMPROVED QC METHODOLOGY

The improved QC scheme is based on the detection of outliers for each grid box and every channel on the remapped antenna temperature files. This procedure was performed based on standardized temperature which use the mean (μ) and standard deviation (σ) in each grid box for the period 1992-2007. The outlier points are defined as those points beyond 10 times the standard deviation for one channel or 6σ for four channels or more (see details in Vila et al, 2010)

3. THE HISTOGRAM MATCHING APPROACH

Histogram matching is a process where a time series, image, or higher dimension scalar data (SSMI/S antenna temperature, in this case) is modified such that its histogram matches that of another reference dataset (SSM/I antenna temperature) (Gonzalez et al, 1992). In this particular application, seven channels of the SSM/I sensor were "matched" with the correspondent channels in the SSMI/S array.

The algorithm is as follows. The cumulative histogram is computed for each dataset (see Figure 1). For any particular value (x_i) in the data to be adjusted has a cumulative histogram value given by $G(x_i)$. This in turn is the cumulative distribution value in the reference dataset, namely $H(x_j)$. The input data value x_i is replaced by x_j. In practice, we create Look-up Tables (LUTs) with the SSMI/S value for each channel and the correspondent output SSMI temperature (reference) which makes this methodology very fast in terms of computing speed.
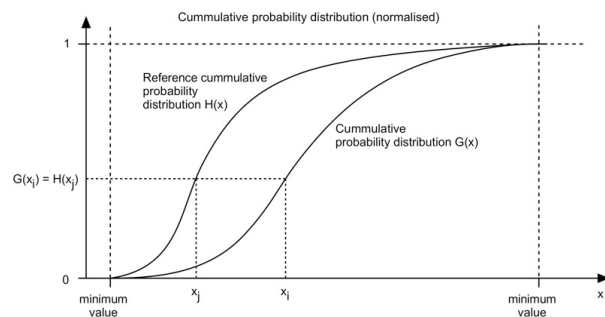

Figure 1: Schematic representation of the histogram matching technique (adapted from http://paulbourke.net/texture_colour/equalisation/)

Because one of the objectives of this study is the continuation of the historical database beginning in 1987 and the use of the existing algorithms for hydrological parameters available for SSM/I, the histogram matching approach appear as a suitable scheme to modify SSMI/S temperatures to match with the SSM/I reference.

In order to achieve this purpose, seven months between January and July 2009 of 1/3 degrees daily grids for SSM/I F-13 and SSMI/S F-17 were chosen to perform this technique. During that period both satellites were flown together with time shift of approximately 1.5 hours. Figure 2 show the PDF (in %) for January 2009 for SSM/I F-13 and SSMI/S F-17 22 GHz Vertical polarization over ocean and over land respectively.
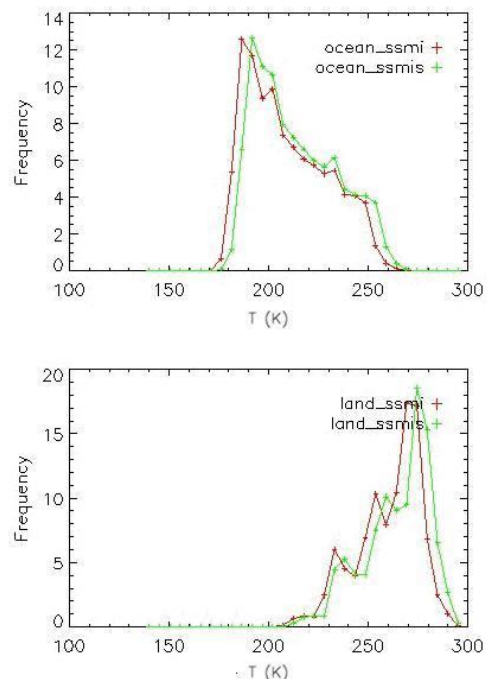

Figure 2: Probability Density Function (in %) for January 2009 for SSM/I F-13 (red line) and SSMI/S F-17 (green line) 22 GHz Vertical polarization over ocean (upper panel) and over land (bottom panel)

It can be seen that both PDFs have a very similar shape but SSMI/S tend to be larger values than SSM/I for this particular channel (22 GHz V). This behavior could be to the fact that there's a time shift between SSM/I and SSMI/S and sensor design.

Look-up tables (LUTs) for every channel (19 GHz H, 19 GHz V, 22 GHz V, 37 GHz V, 37 GHz H, 91/85 GHz V and 91/85 GHz H) stratified for surface type (land & ocean) were created using global 1/3 degree global daily grids for January - July 2009. Those LUTs were applied to SSMI/S

channels and Figure 3 shows the cumulative probability distribution normalized (CPF) for 22 GHz V for August 2009. In this case the red line is SSMI and the green line is the adjusted SSMI/S value. It is important to notice that August 2009 was not used to create the LUTs, so it can be considered as an independent dataset.
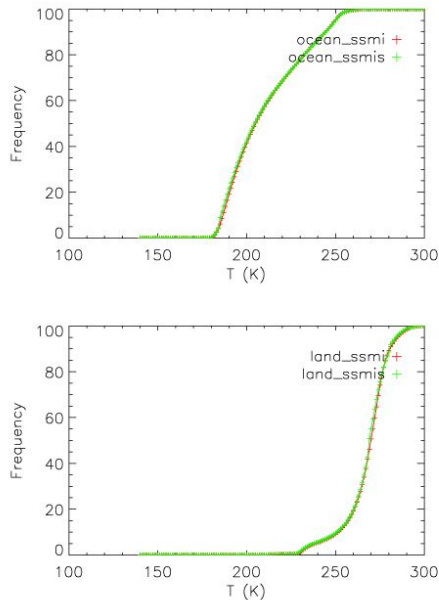

Figure 3: Cumulative Probability Distribution normalized (CPF) for 22 GHz V for August 2009 for SSM/I F-13 (red line) and SSMI/S F-17 (green line) 22 GHz Vertical polarization over ocean (upper panel) and over land (bottom panel)

Similar results can be obtained for other channels (not shown). Figure 4 shows the bias between SSMI/S and SSM/I for 3 different channels (those used for rainfall retrieval: 19 GHz V, 22 GHz V and 91/85 GHz V) for each temperature. While for low frequency channels, the bias is positive (SSMI/S values are larger than SSM/I values) for high frequency channels is the opposite and this bias is larger for lower temperatures (especially over land). The depletion of brightness temperature due the presence of ice is larger for higher frequency (91 GHz) than for 85 GHz. It's also important to notice that this technique is less reliable where few points are present. In the previous figure (Figure 3 - 22 GHz V) it can be seen that few pixels are present for temperatures below 175K over the ocean, so the change of the sign in Figure 4b is not very reliable but it is also not very frequent.
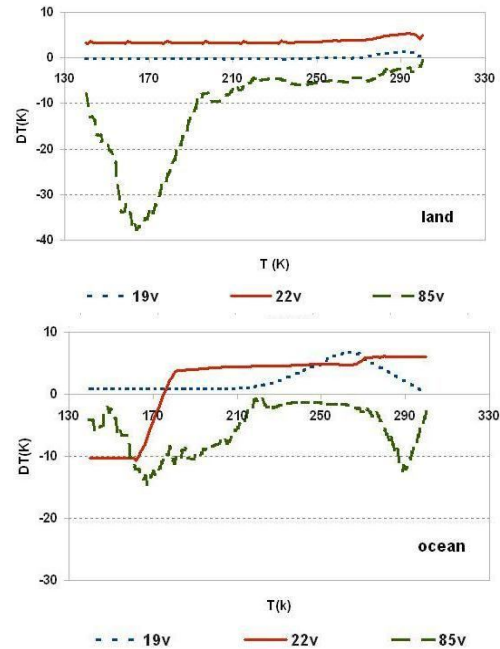

Figure 4: Bias between SSMI/S and SSM/I for 19 GHz V (dashed line), 22GHz V (solid line) and 85 GHz V (long dashed)

4. THE PERFORMANCE OF HYDROLOGICAL MONTHLY PRODUCTS

The first objective of this paper was the reprocessing of the existing SSMI database using an improved QC scheme for antenna temperatures (Vila et al., 2010) for the entire SSMI period (1987-2009). Figure 5 shows the moving average of number of daily pixels on the 1/3 degree antenna temperature images that were excluded using the QC scheme. The mean value for the period 1987-2008 is 1100 pixels per image (per day – ascending node only) which represent less than 1% of the total pixels of a given image.
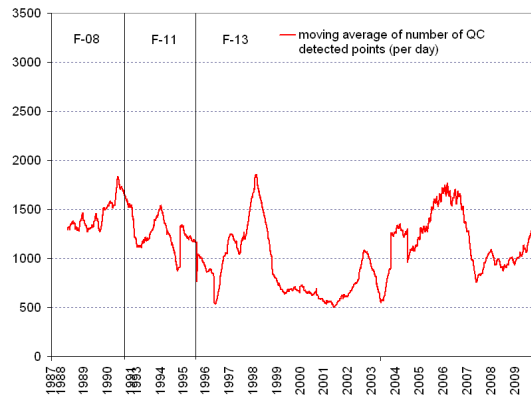
Figure 5: moving average of number of daily pixels in the 1/3 degree antenna temperature images that were excluded using the QC scheme

However, this small amount of pixels can produce an undesirable impact on the monthly products as it is shown in Figure 6. In this case, it is compared the monthly value of a given product before QC and the same values after QC. If this value changes, this pixel is computed as "screened by QC scheme". This change, large or small, is expressed as a percentage of total pixels of the global image.
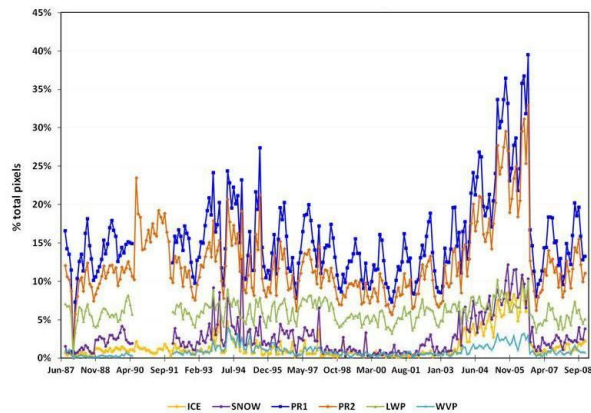

Figure 6: Percentage of pixels screened by QC scheme on monthly basis for sea ice (ICE), snow on the ground (SNOW), precipitation (PR1 and PR2), Liquid Water Path (LWP) and Total Water Vapor (WPV)

This analysis allows studying the sensibility of each product to bad pixels. In the case of PR1 and PR2 (precipitation), the monthly mean is more affected by bad pixels (up to 40% of total amount of pixels differs from non-QC to QC version) while WVP (water vapor) is less affect by bad pixels (below 5%). The sea ice and snow on the ground is a special case because despite of the screened value is below 10%, the total area affected by those surface types is much smaller than the entire globe (large regions of the earth are ice and snow free). It is also important to point out that the maximum in Figure 6 is coincident with a relative maximum in Figure 5.

Once the pixels are detected by QC scheme, it is important to analyze if that screening process has a positive impact on the variables. Figure 7 shows the behavior of precipitation variables (PR1 and PR2) for land over tropical regions when we compare them with independent datasets, In this case, the period from Jan 2004 – Dec 2005 was chosen because, according to Figure 6, a maximum of screened pixels were detected. PR1 and PR2 with QC (dashed lines) are in a better

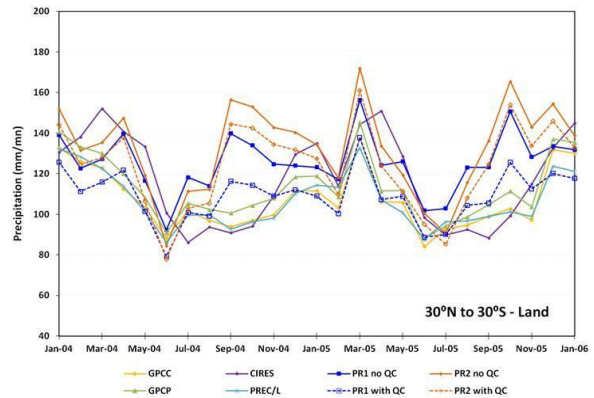agreemen with the rest of the independent dataset (GPCP, GPCC, CIRES and PREC/L) than the non-QC version.

Figure 7: Precipitation variables for land over tropical regions (30°N - 30°S)

The second objective of this paper is to evaluate the performance of hydrological monthly products during SSMI/S era. This era starts in 2006 for late constellation (F15 to F16 transition) and 2009 for early constellation (F13 to F17 transition). As it was mentioned before, this last constellation is particularly important because it is the reference for rainfall retrieval over land for GPCP V2 among other users who also use this information on regular basis. In the next paragraphs we intend to address a comparison between SSM/I and SSMI/S rainfall retrieval during the period where they were flying together (Jan – Nov 2009). Figure 8 shows the histogram for low, medium and high rain rates for August 2009 over land and ocean because this month was not used to create the Look-Up Tables (LUTs). During this month (a similar behavior is observed on other months) the histograms are pretty similar for light and medium rates (the most frequent) and SSMI/S tend to overestimate the rainfall for high rain rates (the less frequent events).
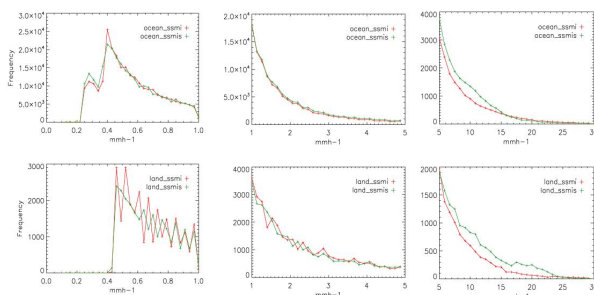

Figure 8: Histogram for light (left), medium (center) and high rain rates (right) over ocean (upper) and land (bottom panel). Red crosses are for SSM/I F-13 and green crosses are for SSMI/S F-17.

However, when the zonal mean for the same month is show (Figure 9), the differences are very small for all latitudes.
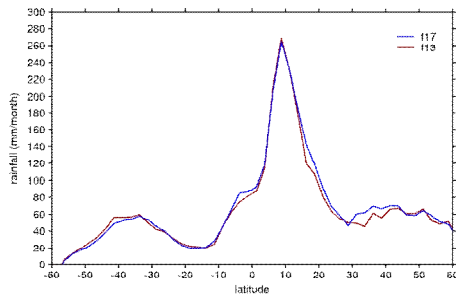

Figure 9: Zonal mean for monthly rainfall in August 2009 for f17 (blue line) and f13 (red line)

Figure 10 shows the monthly rainfall bias for global, ocean and land surfaces for the period Jan 2009-Oct 2009 when both satellite where flying together. With the exception of April 2009, the bias between monthly rainfall estimates for F13 and F17 was below 10% and, most of the cases, below 5%.
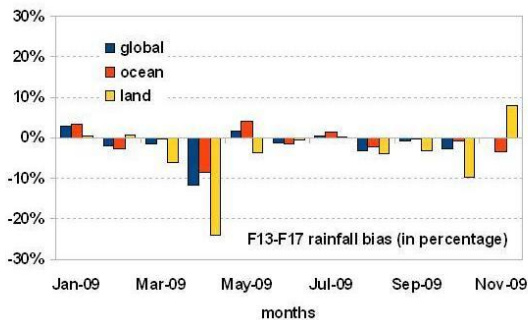

Figure 10: Monthly rainfall bias for global (blue bars), ocean (red bars) and land surfaces (yellow bars) for the period Jan 2009-Oct 2009.

5. REFERENCES

Alihouse J.C., S. Snyder, J. Vongsathorn, and Ferraro R., 1990, Determination of Total Precipitable Water from the SSM/I. *IEEE Trans. Geo. Remote Sensing*, 28 (5), 811-816.

Ferraro R., 1997: Special sensor microwave imager derived global rainfall estimates for climatological applications. *Journal of Geophysical Research-Atmospheres* 102 (D14), 16715-16735.

Gonzalez R. and R. E. Woods. Digital Image Processing. *Addison-Wesley Publishing Company*, 1992, pp. 173-182.

Vila, D., R. Ferraro, and R. Joyce, 2007, Evaluation and improvement of AMSU precipitation retrievals, *J. Geophys. Res.*, 112, D20119, doi:10.1029/2007JD008617.

Vila, D., R. Ferraro, H. Semunegus, 2010: Improved Global Rainfall Retrieval Using the Special Sensor Microwave Imager (SSM/I). *J. Appl. Meteor. Climatol.*, 49, 1032–1043. doi: http://dx.doi.org/10.1175/2009JAMC2294.1